triply bonded nitrogen by a similar amount.

Recently, a set of empirical gas-phase nucleophilicities N and electrophilicities E has been assigned to a series of molecules B and HX, respectively, by taking advantage[28] of a systematic relationship among the hydrogen bond stretching force constants k_σ of a wide range of dimers B···HX. N and E were chosen so as to reproduce the k_σ's through the equation

$$k_\sigma = cNE \quad (7)$$

where $c = 0.25$ N m^{-1}. The E value assigned to HCl was 5.0 and therefore implies, via eq 7, that $N(CH_3NC) = 9.1$, which is very similar in magnitude to $N(CH_3CN) = 8.6$. This result indicates that the n-pairs on isocyano C and cyano N have an essentially identical propensity to interact with the nonperturbing proton donor HCl in the dimers CH_3NC···HCl and CH_3CN···HCl, respectively. The significantly greater proton affinity[26] of CH_3NC than CH_3CN is not, in fact, inconsistent with such a relationship between the N values, for the proton affinity is $\Delta H^\ominus_m$ for the reaction $BH^+ \rightarrow B + H^+$ and the geometries of protonated CH_3CN and CH_3NC are probably quite different. Hence, the proton affinity does not measure just the propensity of the n-pair on the terminal atom to interact with a proton at a fairly long range.

Presumably, the first stage in the rapid reaction of CH_3NC and HCl in the gas phase is the formation of CH_3NC···HCl. It is likely that the next step in the reaction is proton transfer to the carbon atom, but it is not clear whether the reaction is truly homogeneous. It may be that the potential energy barrier to the proton transfer is high in the gas phase but is significantly lowered by surface effects in a heterogeneous reaction.

Acknowledgment. Research grants from the SERC (A.C.L.) and MURST (60%, D.G.L.) in support of this work are gratefully acknowledged.

Registry No. CH_3NC, 593-75-9; HCl, 7647-01-0; $H^{35}Cl$, 13779-43-6; $H^{37}Cl$, 13760-18-4; $D^{35}Cl$, 14986-26-6.

(28) Legon, A. C.; Millen, D. J. *J. Am. Chem. Soc.* **1987**, *109*, 356.

Low-Energy Electron Impact Spectroscopy of [1.1.1]Propellane: Electron Attachment Energies and Singlet and Triplet Excited States

Olivier Schafer,[†] Michael Allan,*[,†] Günter Szeimies,*[,‡] and Maximilian Sanktjohanser[‡]

Contribution from the Institut de Chimie Physique de l'Université Fribourg, CH-1700 Fribourg, Switzerland, and Institut für Organische Chemie der Universität München, Karlstrasse 23, D-8000 München, FRG. *Received April 1, 1992*

Abstract: Electron transmission spectra and energy and angular dependence of vibrational excitation by electron impact were recorded and used to characterize different states of the short-lived negative ion (resonances) of the title compound. The first attachment energy, corresponding to electron capture into the $3a_2''$ LUMO, is 2.04 eV, exceptionally low in comparison with a typical value of ~6 eV for a saturated hydrocarbon. Observation of (faint) vibrational structure indicates a lifetime broadening of the order of a vibrational spacing for this resonance, much less than is typical for σ^* resonances of saturated hydrocarbons (several electron volts). The Frank-Condon width of the band, 0.6 eV (fwhh), and intense excitation of ν_3 vibrational mode point to appreciable lengthening of the interbridgehead distance (R_{bb}) in the negative ion. Additional, higher-lying and broad σ^* resonances with maxima around 6-7 eV are observed in vibrational excitation functions, and a core exited $^2(5a_1',3a_2''^2)$ resonance is observed at 7.36 eV in the excitation function of the lowest triplet state. Electron energy loss spectra in the electronic excitation energy range reveal the triplet and singlet excited states. The vertical excitation energy to the lowest triplet state is 4.70 eV, also exceptionally low for a saturated hydrocarbon and in line with the low energy of the LUMO. A long progression in the C-C stretch vibration ν_3 indicates appreciable lengthening of R_{bb} in the triplet state. An intense dipole allowed transition to the lowest valence singlet state is found at 7.26 eV. The band is unusually narrow and the state is proposed to have partly Rydberg character. The spectra further reveal several Rydberg states and Feshbach resonances.

I. Introduction

The successful synthesis of [1.1.1]propellane (**1**), a truly remarkable hydrocarbon with "inverted" geometries at the bridgehead carbon atoms, has opened the way to numerous experimental (and more theoretical) studies of its properties.[1] The structure,[2] vibrational spectrum, and heat of formation have been determined.[3] The compound was found to be remarkably stable and to have a surprisingly short bridge length (160 pm, only ~9 pm longer than in cyclopropane), unexpected in view of the extreme deviation from tetrahedral geometry and the intuitively anticipated strain. These findings initiated a series of theoretical studies on the nature of the bridging bond.[4] A photoelectron spectrum[5] of **1** revealed a remarkably narrow first band, indicating only a minute, (for saturated hydrocarbons atypical) change of

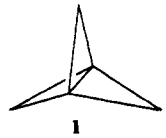

1

[†] Université Fribourg.
[‡] Universität München.

(1) Wiberg, K. B. *Acc. Chem. Res.* **1984**, *17*, 379.
(2) Hedberg, L.; Hedberg, K. *J. Am. Chem. Soc.* **1985**, *107*, 7257.
(3) Wiberg, K. B.; Dailey, W. P.; Walker, F. H.; Waddell, S. T.; Crocker, L. S.; Newton, M. *J. Am. Chem. Soc.* **1985**, *107*, 7247. K. Wiberg, private communication.
(4) Slee, T. S. In *Modern Models of Bonding and Delocalization*; Liebman, J. F., Greenberg, A., Eds.; VCH Publishers: New York and Weinheim 1988; pp 63-114. Wiberg, K. B.; Bader, R. F. W.; Lau, C. D. H. *J. Am. Chem. Soc.* **1987**, *109*, 985.
(5) Honegger, E.; Huber, H.; Heilbronner, E.; Dailey, W. P.; Wiberg, K. B. *J. Am. Chem. Soc.* **1985**, *107*, 7172.

0002-7863/92/1514-8180$03.00/0

geometry upon ionization. This observation is supported by calculations for **1** and $\mathbf{1}^+$. Although this would seem to imply a nearly nonbonding HOMO of **1**, caution regarding this interpretation in the case of **1** has been recommended in view of the tight cage structure of the molecule.[5]

The experimental information on the virtual orbitals of **1** is much more scarce, limited to few theoretical predictions.[6,7] It has been pointed out[7] that the $3a_2''$ orbital has a considerable amount of bridgehead–nonbridgehead density and is not simply the antibonding version of $5a_1'$ HOMO. Few predictions have been made concerning the excited states of **1**. Early calculations located the $^3A_2''$ state at ~2 eV.[8] More recent SCF MP3 calculations resulted in the value of 3.2 eV at the optimal geometry, corresponding to a much longer bridgehead–bridgehead distance (R_{bb}) of 183 pm.[3] Potential energy curves for the $(5a_1',3a_2'')$ $^3A_2''$ and $^1A_2''$ states as a function of R_{bb} predicted[7] a considerable singlet–triplet separation and a large R_{bb} lengthening in the triplet, but nearly no change in R_{bb} in the singlet state.

We wish to extend the experimental work done on this exciting molecule, applying to it various low-energy electron impact spectroscopic methods,[9] in order to obtain experimental information on the properties of the short-lived radical anions, which are related to the virtual orbitals of **1**, and in order to obtain additional information on the singlet and triplet excited states.

The methods comprise electron transmission spectroscopy (ETS),[10] whose application to chemistry has been pioneered by Burrow and Jordan.[11] It reveals short-lived states of the radical anion (synonymously called "resonances in electron–molecule scattering" or just "resonances") as variations in total electron scattering cross section. Measurements of the energy dependence of the differential cross sections for vibrational and electronic excitation provide a refined means to study the resonances and their properties,[12] especially in organic molecules.[13] Electron energy loss spectroscopy (ELS) is capable of revealing spin and dipole forbidden electronic transitions.[14]

This work concentrates on the aspects of the electron impact spectra relevant to understanding the electronic structure of **1**. An account emphasizing a more detailed understanding of the electron scattering process, and including absolute values of the differential cross sections, is planned for a later publication. The entire electron impact study, in particular, the cross-beam part, required about 0.5 g of neat sample and would not be possible without advances in the synthesis of **1**.

II. Experimental Section

The trochoidal electron spectrometer[15] and the electrostatic spectrometer[16] used in the present study have already been described and only a brief description is given here. The first instrument measures both ET spectra and EL spectra; the second is an energy loss spectrometer. The two instruments are complementary in the EL mode. The first is much more sensitive and thus particularly suitable for measurements of the weak electronic excitation; the second permits variation of the scattering angle, measurements of even small vibrational energy losses, and has a somewhat higher resolution.

The trochoidal electron spectrometer focuses the electron beam by an axial magnetic field and uses trochoidal monochromators[17] both to prepare a quasi-monoenergetic incident electron beam and to analyze the energies of the scattered electrons. This spectrometer operates at a fixed scattering angle, and the data obtained are superposition of 0° and 180° differential cross sections since this instrument detects both forward and backward scattered electrons simultaneously. The excitation functions

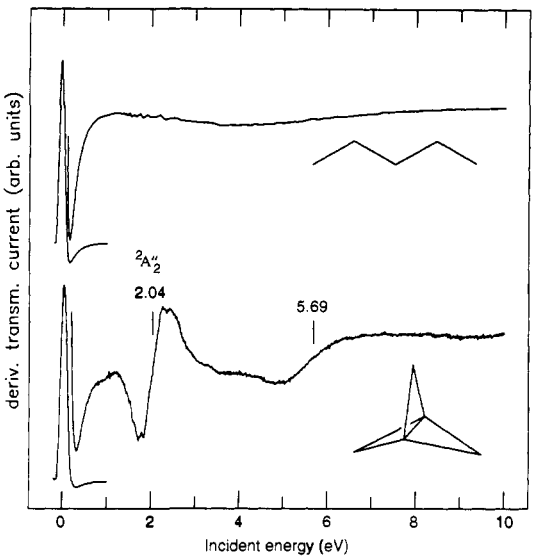

Figure 1. Electron transmission spectra of [1.1.1]propellane and *n*-pentane. The deep dips at 0.2–0.3 eV in both spectra are due to nonresonant variations of the cross sections, probably mainly to the Ramsauer–Townsend minimum. Weak narrow structures at 1.5–2.5 eV in both spectra are caused by the "focusing" artifact of an ET instrument. Two resonant features in the lower spectrum are marked by vertical lines and vertical attachment energies.

are corrected for the instrumental response function determined on the He ionization continuum. The analyzer electrodes are short-circuited and used as a collector for the transmitted electron beam in the ET mode. The sample was kept at −40 °C and the vapor introduced into a collision chamber through a needle valve.

The electrostatic instrument uses hemispherical deflectors to prepare a beam of quasi monoenergetic electrons and to energy-analyze the scattered electrons. The analyzer is rotatable from −3° to 135° with respect to the incident beam, and the instrument measures differential cross sections. The sample was kept at −15 °C and its vapor introduced through a 30-μm nozzle into the collision region (the backing pressure is too low to cause any noticeable cooling or clustering by supersonic expansion, however). The instrumental response function with respect to angle and electron energy was calibrated by comparing the elastic e–He signal with established calculated cross-section values.[18]

[1.1.1]Propellane (**1**) was prepared free of solvent from 1,3-diiodobicyclo[1.1.1]pentane by reaction with 2.0 equiv of sodium cyanide in dimethyl sulfoxide following the recently published procedure.[19]

III. Results

Transmission Spectrum. Transmission spectra of saturated hydrocarbons, exemplified by the spectrum of *n*-pentane in Figure 1, are in general characterized by the absence of discernible resonances, the anionic states associated with σ^* orbitals being high in energy and too broadened by their excessively short lifetimes to be distinguishable from the "natural" variations of nonresonant scattering. Exceptions to this rule are ET spectra of some cyclic hydrocarbons with distinguishable, albeit relatively high-lying (5.3 eV in cyclopropane, 4.1 eV in cyclohexane) and broad resonances.[20] The spectrum of **1** in Figure 1 is thus truly remarkable for a saturated hydrocarbon and resembles somewhat the spectrum of ethene.[11] The well-developed band at 2.04 eV may be assigned to a temporary capture of the incoming electron into the LUMO $3a_2''$ (disregarding configuration mixing, which is not expected to play a dominant role in this case because of the relatively large energy gap to the higher-lying configurations). A second, broader and less distinct feature is seen at 5.69 eV. Even this feature is narrower than any features in *n*-pentane; its energy and width resemble those found in the ET spectrum of cyclopropane.[20] It will be discussed in more detail below.

Vibrational Excitation. Nonresonant vibrational excitation by electron impact is usually very weak,[12] except for IR-allowed

(6) Jackson, J. E.; Allen, L. C. *J. Am. Chem. Soc.* **1984**, *106*, 591.
(7) Feller, D.; Davidson, E. R. *J. Am. Chem. Soc.* **1987**, *109*, 4133.
(8) Newton, M. D.; Schulman, J. M. J. *J. Am. Chem. Soc.* **1972**, *94*, 773.
(9) Schafer, O. Thèse de docteur ès sciences naturelles, Fribourg, 1992.
(10) Sanche, L.; Schulz, G. J. *Phys. Rev. A* **1972**, *5*, 1672.
(11) Jordan, K. D.; Burrow, P. D. *Acc. Chem. Res.* **1978**, *11*, 341. Jordan, K. D.; Burrow, P. D. *Chem. Rev.* **1987**, *87*, 557.
(12) Schulz, G. J. *Rev. Mod. Phys.* **1973**, *45*, 423.
(13) Walker, I. C.; Stamatovic, A.; Wong, S. F. *J. Chem. Phys.* **1978**, *69*, 5532.
(14) Kuppermann, A.; Flicker, W. M.; Mosher, O. A. *Chem. Rev.* **1979**, *79*, 77.
(15) Allan, M. *J. Electron Spectr. Relat. Phenom.* **1989**, *48*, 219–351.
(16) Allan, M. *J. Phys. B: At. Mol. Opt. Phys.* **1992**, *25*, 1559.
(17) Stamatovic, A.; Schulz, G. J. *Rev. Sci. Instrum.* **1968**, *39*, 1752.
(18) Nesbet, R. K. *Phys. Rev. A* **1979**, *20*, 58.
(19) Alber, F.; Szeimies, G. *Chem. Ber.* **1992**, *125*, 757.
(20) Howard, E.; Staley, S. W. *ACS Symp. Ser.* **1984**, *263*, 183.

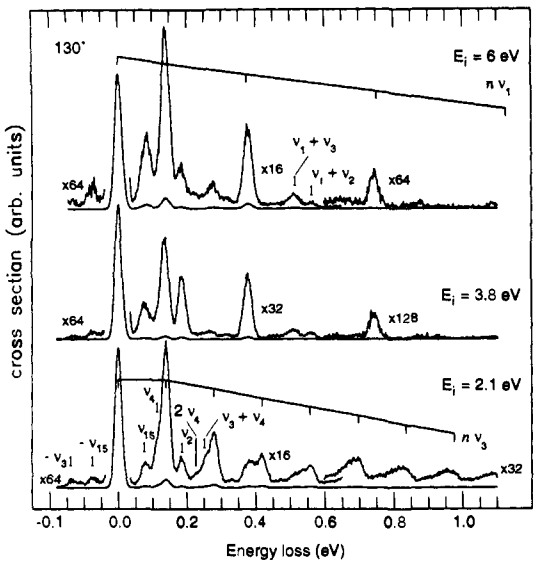

Figure 2. Vibrational energy loss spectra recorded at 130° and three incident energies. The energies of selected vibrational levels are indicated. The three curves are not on the same vertical scale, and multiplication factors indicate vertical expansion with respect to elastic peaks.

Table I. Vibrations of [1.1.1]Propellane Relevant to the Present Paper (from Ref 3)

mode		E (meV)	IR int	approximate description
A_1'	ν_1	376		sym C–H stretch
	ν_2	186		HCH scissor
	ν_3	139		sym R_{bb} and R_{bm} C–C stretch[a]
	ν_4	113		sym R_{bb} and R_{bm} C–C stretch[b]
E'	ν_8	374	s	C–H stretch
	ν_9	181	m	C–H bend (and R_{bb} and R_{bm} stretch)
A_2''	ν_{14}	136	m	HCH rocking
	ν_{15}	76	vs	asym R_{bm} C–C stretch

[a] Variations of R_{bb} and R_{bm} are in phase. [b] Variations of R_{bb} and R_{bm} are out of phase.

transitions which are appreciably excited by dipole interaction, mainly in forward scattering and low energies (adequately described by the Born dipole approximation[21]). On the other hand, temporary negative ion states cause the nuclei to move, for a short time, on a potential different from that of the neutral molecule, and often induce appreciable excitation of certain, most often totally symmetric vibrations. The dependence of the vibrational excitation cross section on incident energy thus represents a convenient means to study the resonances.

A resonance may be thought as imparting an impulse to the nuclei in the direction of the slope of the anionic potential hypersurface, i.e., along bonds which are appreciably lengthened (or shortened), or with respect to bond angles changed by the capture of the incoming electron. This impulse leads to excitation of vibrations involving corresponding coordinate changes, the intensity of excitation reflecting the degree of change in the geometry, and the lifetime of the resonance and thus duration of the force impact. The force field has the symmetry of the symmetrized square of the irreducible representation of the negative ion involved and can excite only vibrations of this symmetry.[22,23] Application of this symmetry rule to nondegenerate resonances such as the lowest $^2A_2''$ resonance in **1** reveals that only the four totally symmetric vibrations[3] ν_1–ν_4 may be excited. Which of these vibrations will actually be excited and to what degree is determined by the difference between the geometry of the neutral molecule and that of the intermittent negative ion. Determination of the selectivity of vibrational excitation thus allows conclusions about the bonding in the temporary negative ion and indirectly the bonding properties of the temporarily filled orbital.

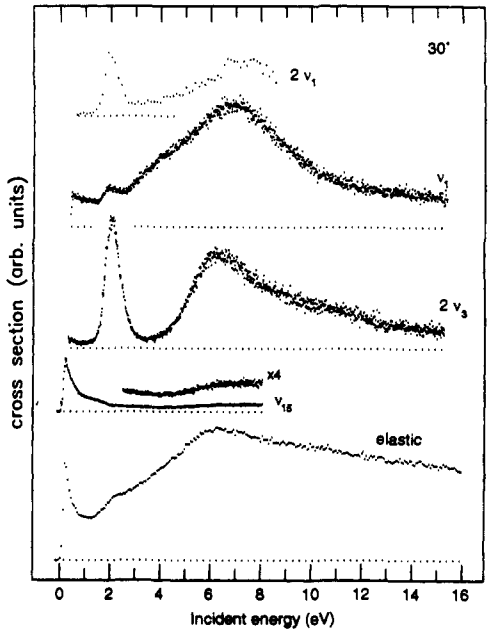

Figure 3. Excitation functions for the elastic and four vibrationally inelastic peaks at 30°. The curves are not on the same vertical scale.

Figure 2 shows vibrational energy loss spectra of **1**. Properties of the vibrations relevant in this work are summarized in Table I. The most striking feature in the spectrum obtained with an incident energy of 2.1 eV, where excitation is enhanced by the $^2A_2''$ resonance, is a long progression in the ν_3 vibration. Normal coordinate analysis[3] reveals changes in the molecular coordinate R_{bb}, and to a lesser degree R_{bm} (bridgehead carbon to methylene carbon distance), as dominating the ν_3 vibration. The long progression in ν_3 is thus in good accord with the picture of this vibration being excited by a substantial lengthening of R_{bb} during the lifetime of the resonance, expected from the fact that the LUMO $3a_2''$ has a node crossing R_{bb}. An interesting detail concerns the fact that ν_3 is excited more strongly than ν_4, although both vibrations involve a large stretch of the R_{bb} distance. This observation, together with the calculated result[3] that the R_{bb} and R_{bm} motions are in phase in ν_3 and out of phase in ν_4, indicates that both R_{bb} and R_{bm} are lengthened in the negative ion. This observation appears to be in contradiction with a naive interpretation of the bonding density of the LUMO $3a_2''$ along R_{bm}, but confirms the result of a more elaborate calculation, discussed in section IV.

The excitation of the $2\nu_3$ overtone shown in Figure 3 experiences great enhancement by the $^2A_2''$ resonance. The derivative of a long acquisition of the $2\nu_3$ signal in the $^2A_2''$ resonance region reveals very weak vibrational structure with spacing of ~110 meV. The presence of structure, albeit weak, indicates lifetime broadening which is not large relative to vibrational spacing, so that most of the observed width of the band, 0.6 eV fwhh (full width at half-height), must be due to the width of the Franck–Condon profile. For comparison, the fwhh of the first PE band is only 0.2 eV (see ref 5 and text below). The occupation of the LUMO $3a_2''$ thus causes a much larger change of molecular geometry than the ionization from the HOMO $5a_1'$. The relatively long lifetime of the 2.1-eV resonance is also reflected in its capacity to excite very high vibrational overtones, exemplified by the excitation of $10\nu_3$ in Figure 4. The 6.3-eV resonance leads to only little $10\nu_3$ excitation, probably because of its short lifetime. The 2.1-eV peak is slightly narrower in the $10\nu_3$ decay channel than in the $2\nu_3$ channel. This trend is not unusual in electron scattering and has an analogy already in the diatomic molecules N_2 and CO (see ref 15 for sample spectra), where it has been well reproduced by theory.

The angular distribution of the vibrationally inelastically scattered electrons is informative of the symmetry of the scattering

(21) Itikawa, Y. *J. Phys. Soc. Jpn.* **1974**, *36*, 1121.
(22) Wong, S. F.; Schulz, G. J. *Phys. Rev. Lett.* **1975**, *35*, 1429.
(23) Gallup, G. A. *Phys. Rev. A* **1986**, *34*, 2746.

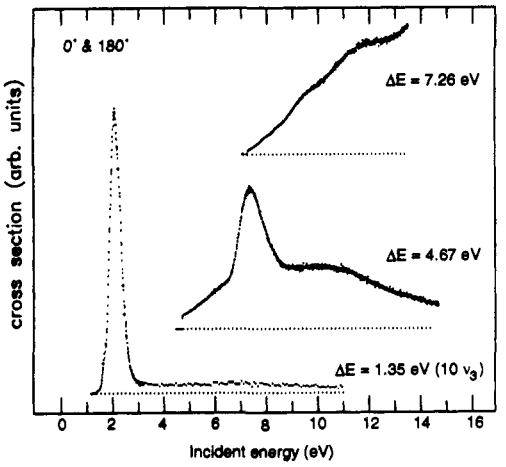

Figure 4. Excitation functions for a deeply vibrationally inelastic and two electronic excitation peaks measured with the trochoidal spectrometer (superposition of 0° and 180°). The curves are not on the same vertical scale. The shallow oscillatory deviations from linearity in the upper trace are probably of instrumental origin.

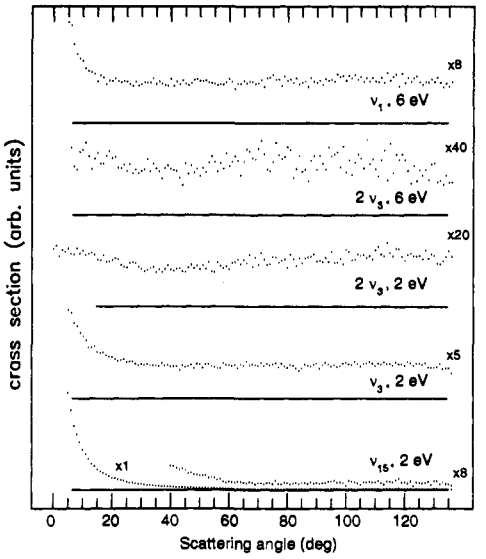

Figure 5. Angular dependences for different energy loss peaks and at two different incident energies. All curves are on the same relative scale, vertically offset as indicated by solid horizontal lines, and expanded vertically as indicated by multiplication factors.

state,[12,13,24,25] and we therefore show representative angular distributions obtained with the present compound in Figure 5. The angular distribution of electrons having excited the $2\nu_3$ overtone is not far from isotropic, with only a shallow minimum around 40°. Visual inspection of the shape of the LUMO $3a_2''$ indicates that the scattering will not be dominated by a single partial wave, but that both p_σ and f_σ will be important, with a possible s_σ contribution in the exit channel made possible by simultaneous rotational transitions. The resulting angular distribution is then a function of the mixing coefficients and phases[24] of the individual contributions, which cannot be easily determined, preventing a simple prediction of the angular distribution. We note, however, that the f_σ angular distribution has a minimum around 40°, and the observed angular distribution thus does not contradict our assignment of the resonance.

The behavior of the energy loss peak for ν_{15} at 75 meV in Figure 2 is characteristic for direct dipole excitation of an IR-active vibration, that is, the energy dependence peaks near excitation threshold (Figure 3) and angular dependence peaks at 0° (Figure 5). It is assigned to excitation of the ν_{15} vibration, which is also responsible for the most intense IR band.[3] The energy and angular dependence data in Figures 3 and 5 provide evidence for direct excitation of other IR-active vibrations. The IR-active fundamental ν_{14} overlaps with ν_3 and causes signal rise at low angles in the curve labeled as ν_3 angular dependence in Figure 5; the also IR-active ν_8 overlaps with ν_1 and causes the rise of the corresponding signal with decreasing energy below 2 eV in Figure 3 and at low angles in Figure 5. The overlap of IR-active and totally symmetrical vibrations thus makes the excitation functions of the fundamental frequencies less suitable for detecting resonances; in contrast the excitation functions of the $2\nu_3$ and $2\nu_1$ overtones in Figure 3 are free of nonresonant signal.

A further vibrational feature attracting attention in Figure 2 is a progression in the excitation of a C–H stretch vibration, particularly at 6 eV. We assign it to the excitation of the totally symmetric vibration $n\nu_1$ (except for some overlap of $1\nu_1$ and IR active $1\nu_8$ at low scattering angles and low energies as explained above). The $n\nu_1$ excitation functions are also enhanced by the $^2A_2''$ resonance, but are dominated by a very broad band peaking at 6.9 eV (Figure 3). This feature of C–H stretch excitation has a parallel in virtually all compounds containing C–H bonds[13,15,26,27] and is usually assigned as due to "σ^*" resonances.

There is further a peak at $\Delta E = 185$ meV in Figure 2, labeled ν_2 for simplicity, although it may also contain contribution from the IR-active vibration ν_9. This energy loss peak is excited to some degree at all incident energies, with a weak enhancement at 2 eV and a broad enhancement peaking around 7 eV.

This section is concluded by the discussion of several finer details of the vibrational spectra. There is a shoulder on the low-energy side of the $1\nu_3$ peak in the $E_i = 2.1$ eV spectrum in Figure 2, which can be assigned as the totally symmetric vibration ν_4, also involving stretch of R_{bb} and R_{bm}. Two shoulders left of the $2\nu_3$ peak can be assigned as $2\nu_4$ and $\nu_3 + \nu_4$. All higher $n\nu_3$ peaks appear asymmetrically broadened toward lower ΔE, and this broadening can be interpreted as resonant excitation of $i\nu_3 + j\nu_4$ combination vibrations with $i + j = n$, which all lie to the left of the $n\nu_3$ peaks.

The intensity of the ν_{15} excitation in Figure 5 first drops with increasing scattering angle, but remains nearly constant above 60°, indicating that a resonant excitation mechanism is also active in addition to the direct dipole excitation. Two possible explanations may be forwarded for this resonant excitation. First, it has been pointed out that vibronic coupling between resonances leads to excitation of nontotally symmetrical vibrations.[28] The a_2'' vibration ν_{15} could be excited by coupling of the $^2A_2''$ resonance with a higher-lying $^2A_1'$ resonance. Virtual orbitals with a_1' symmetry are calculated at higher energies as will be discussed below, making this assumption reasonable. In fact, both a_1' and a_2'' virtual orbitals are calculated at higher energies, opening the possibility of explaining the enhanced excitation of ν_{15} near 6 eV (Figure 3). Secondly, it has been pointed out by Gallup[23] that the departing electron may appear in a different partial wave than the incident electron and that in such case s-wave outgoing electrons will be important at low energies. The vibrations excited will then be of the same symmetry as the resonance, a_2'', that is, ν_{14} and ν_{15} for propellane at 2.1 eV. Of these two, ν_{15} is expected to be more important, since it involves strong changes in C–C bond lengths.

The signal to the left of the elastic peak is due to superelastic scattering on thermally vibrationally excited molecules. Vibrational cross sections were recorded up to 25 eV, and no bands other than those seen in Figure 3 were observed.

Electronic Excitation. Energy loss spectra at three representative energies are shown in Figure 6. Some of the features, the broad structured band at 2 eV and the sharp peaks in the 6–6.5-eV range marked F_1 and F_2, all in the $E_r = 0.1$ eV spectrum, are identified as due to "nearly horizontal" decay of the $^2A_2''$ shape

(24) Read, F. H. *J. Phys. B* **1968**, *1*, 893. Andrick, D.; Read, F. H. *J. Phys. B: At. Mol. Phys.* **1971**, *4*, 389.
(25) Stephen, T. M.; Burrow, P. D. *Chem. Phys. Lett.* **1991**, *179*, 252.
(26) Tanaka, H.; Kubo, M.; Onodera, N.; Suzuki, A. *J. Phys. B: At. Mol. Phys.* **1983**, *16*, 2861.
(27) Andric, L.; Hall, R. I. *J. Phys. B: At. Mol. Opt. Phys.* **1988**, *21*, 355.
(28) Estrada, H.; Cederbaum, L.; Domcke, W. *J. Chem. Phys.* **1986**, *84*, 152.

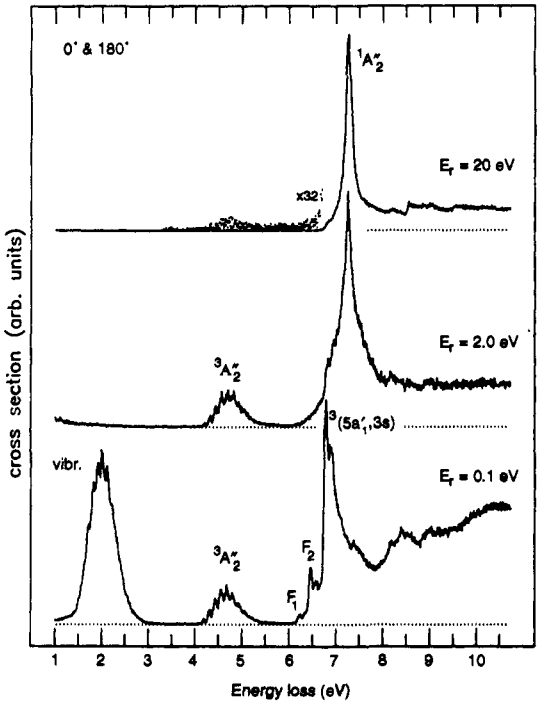

Figure 6. Extended range energy loss spectra, recorded with the trochoidal spectrometer at the three constant residual energies indicated. The peak at ΔE = 2 eV in the bottom spectrum is due to excitation of high vibrational levels of the electronic ground state, mediated by the $^2A_2''$ resonance, the peaks labeled F_1 and F_2 to decay of Feshbach resonances, the remaining peaks to electronic excitation.

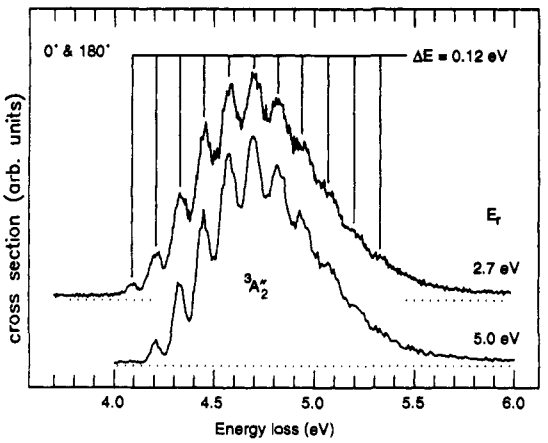

Figure 7. Expanded view of the $^3A_2''$ energy loss band. The residual energy of 2.7 eV corresponds to excitation via the 7.36-eV core-excited resonance (see Figure 4), enhancing the lower vibrational levels.

resonance at 2.04 eV and of sharp Feshbach resonances at 6.34 and 6.57 eV by the fact that they remain fixed to a given incident energy when the residual energy is changed.[15,29] The remaining features are transitions to electronically excited states.

The structured band at 4.7 eV has an energy dependence (Figure 4) characteristic of a transition to a triplet state, and we assign it to the valence (5a$_1'$,3a$_2''$) $^3A_2''$ state. An expanded view of this band can be found in Figure 7. The large width indicates a large change in geometry in agreement with theoretical predictions.[7] The vibrational structure is dominated by a long progression in a single vibration with a mean spacing of 0.12 eV (980 ± 40 cm^{-1}). We propose the assignment of this vibration to ν_3 (0.139 eV in the ground state) on the grounds of the geometry distortion in the triplet state being given mainly by the antibonding properties of the 3a$_2''$ MO, which, when singly occupied in the ground state of the anion, leads primarily to excitation of $n\nu_3$

(29) Allan, M. Int. J. *Quant. Chem.* **1987**, *31*, 161.

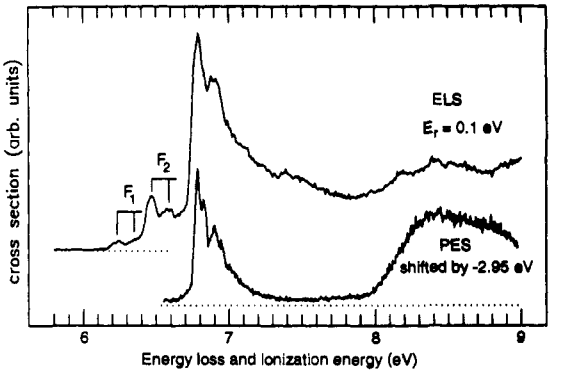

Figure 8. Expanded view of an energy loss spectrum in the Rydberg excitation region and the photoelectron spectrum, shifted in energy to permit convenient comparison of the band shapes.

(preceding section). The observed energy is in satisfactory qualitative agreement with theoretical predictions.[3,7,8]

The enhancement at 7.36 eV in the excitation function of the triplet state (Figure 4) has an analogy in the excitation functions of triplet states in many other compounds[15] and may be assigned to the ^{2}(5a$_1'$,3a$_2''^2$) core-excited resonance, in which the 3a$_2''$ LUMO is doubly occupied. The $^3A_2''$ triplet state is the parent state of this resonance and this decay channel is therefore favored. It is interesting to note that the low vibrational levels of the $^2A_2''$ state are enhanced in the upper curve of the spectrum in Figure 7, where the excitation occurs via the core-excited shape resonance. This deviation from the Franck–Condon profile is explained as a consequence of nuclear relaxation during the lifetime of the resonance. It indicates that the core-excited resonance is distorted along the same "direction" as the $^3A_2''$ excited state, supporting the notion of the same orbital, the 3a$_2''$ LUMO, being occupied in both the resonance and the triplet state.

The next band, observed at 6.79 eV in the energy loss spectra, also nearly disappears at E_r = 20 eV and may be attributed to a triplet state. A comparison with the shape of the photoelectron band, shown in Figure 8, identifies it as a Rydberg state converging to the first ionization energy. The quantum defect of δ = 0.85 eV finally leads to the assignment as ^{3}(5a$_1'$,3s) $^3A_1'$. A weak feature at 6.95 eV in the spectra with E_r = 0.3 to 1 eV (not shown) has the correct energy and dependence on E_r to correspond to the dipole forbidden transition to the ^{1}(5a$_1'$,3s) $^1A_1'$ Rydberg state. Inspection of Figure 8 further suggests transition to the ^{3}(1e'',3s) $^3E''$ Rydberg state, converging to the second ionization energy, as an assignment for the broad feature between 8.1 and 8.7 eV in the energy loss spectrum. Note that the first PE band in Figure 8 confirms the observation of a very low frequency vibration originally reported in ref 5, where the authors propose that the explanation of its excitation could be looked for in vibronic mixing.

The next feature (7.26 eV) in the energy loss spectra (Figure 6, E_r = 20 eV) is a remarkably narrow peak (0.16 eV fwhh), without vibrational structure discernible with the present resolution. Its behavior with residual energy reveals it to be a result of a dipole allowed transition to a singlet state. Its assignment to a ^{1}(5a$_1'$,3s) $^1A_1'$ Rydberg state is not satisfactory since this transition is dipole forbidden and the band shape differs too much from the band shape of the corresponding PES and triplet Rydberg bands. Also the energy separation from the latter, 0.47 eV, is too large for a typical singlet–triplet separation of 3s Rydberg states in hydrocarbons (e.g. 0.05 eV in benzene[15]). The band-shape argument also speaks against a (5a$_1'$,3p) assignment. We propose that the band corresponds to the dipole allowed HOMO–LUMO transition to the $^1A_2''$ state. The band appears intuitively too narrow for a valence transition, but the geometries of the ground and the $^1A_2''$ excited states were theoretically predicted to be nearly identical.[7] The narrow width could in addition be taken as an indication of some Rydberg character of the 3a$_2''$ orbital in this state, rendering it essentially nonbonding.

The spectrum with E_r = 2 eV in Figure 6 gives evidence for a second valence triplet state in the form of structureless signal

Table II. Observed Vertical Attachment Energies (Band Maxima, in eV, ±0.04 eV for Narrow Features)

energy	vibr spacing	assignment
2.04	~0.11	$^2A_1''$ $^2(3a_2'')$ shape
6.3		σ^{*a}
6.8		σ^{*b}
6.33	0.11_5	$^2(5a_1',3s^2)$ Feshbach
6.57	0.11_5	$^2(5a_1',3s3p)$ Feshbach
7.36		$^2(5a_1',3a_2''^2)$ core-excited shape

[a] Broad band in ν_3 (C–C stretch) excitation function. [b] Broad band in ν_1 (C–H stretch) excitation function.

Table III. Observed Transition Energies (Band Maxima, in eV, ±0.02 for Sharp Features)

energy	vibr spacing	assignment
4.69_5 (4.09)[a]	0.12	$^3A_2''$ $^3(5a_1',3a_2'')$
~6.7		$^3E'$ $^3(1e'',3a_2'')$
6.79	0.11	$^3(5a_1',3s)$ Rydberg
6.95		$^1(5a_1',3s)$ Rydberg
7.26		$^1A_2''$ $^1(5a_1',3a_2'')$
8.4		$^{1,3}(1e'',3s)$ Rydberg

[a] First observed vibrational level (probably $\nu = 0$) in parentheses.

which has an onset around 6.2 eV and becomes obscured by the Rydberg states above 6.8 eV. This state is about 2 eV above the $^3A_2''$ state, this energy being of similar magnitude as the separation of the e'' and a_1' occupied molecular orbitals. We therefore propose the assignment $^3(1e'',3a_2'')$ $^3E'$ for this band.

Summary of the observed attachment and transition energies is given in Tables II and III.

IV. Discussion

It has been established that the attachment energies may be rationalized by correlation with SCF energies of virtual orbitals for large molecules,[30,31] where full scattering calculations are not possible. For example, a least-squares fit between experimental attachment energies and the orbital energies ϵ obtained with the 6-31G basis resulted in the linear scaling relation[32] AE = $(\epsilon - 2.33)/1.31$ (eV).

Figure 9 shows MO energies of **1** calculated with the Gaussian 90[33] program, together with a schematic representations of four selected orbitals. Using the above scaling relation, we obtain 1.5 eV as an expectation value for the first AE, in qualitative agreement with the experimental value despite the fact that the scaling relation was not calibrated on σ^* resonances. Visual inspection of the HOMO and the LUMO reveals that the former is bonding and the latter antibonding with respect to the R_{bb} distance to about the same degree. This does not allow for a qualitative rationalization of the observed small geometry change upon ionization and large geometry change upon electron attachment. Complete geometry optimization of the cation did, however, correctly reproduce the nearly zero change of geometry.[5] Geometry optimization of an autodetaching negative ion with standard quantum chemical programs is somewhat controversial because the variational principle does not apply and the "extra" electron is artificially held in the vicinity of the molecule by the finite size of the basis set. On the other hand, the procedure is expected to give useful results despite this problem, since the wave function for the "bound" state part of the shape resonance will have appreciable amplitude only within the angular momentum barrier, close to the nuclei.[32] We optimized the geometry for the

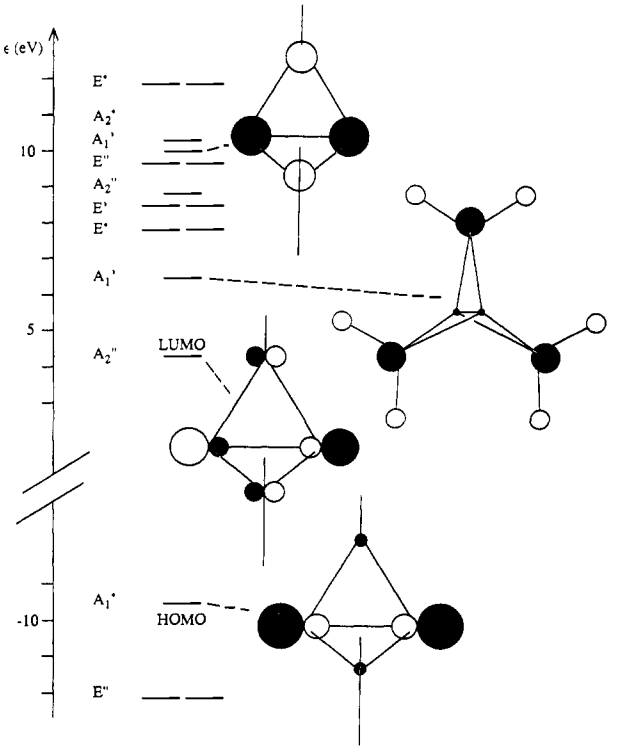

Figure 9. Energies of high-lying filled and low-lying unfilled orbitals of [1.1.1]propellane, calculated with the Gaussian 90 program using a 6-31G basis set. Schematic diagrams of four selected MO's, drawn with the program Moplot,[35] is also shown.

negative ion at the UHF/6-31G** level and obtained a R_{bb} distance of 188 pm and R_{bm} distance of 155 pm. This amounts to a substantial lengthening of R_{bb} and a small lengthening of R_{bm} with respect to the neutral molecule, in agreement with the indication derived above from the vibrational excitation results. (R_{bb} was calculated to be 154 pm and R_{bm} 150 pm in the neutral molecule at the HF/6-31G** level, in reasonable agreement with the experimental values of 160 pm and 152 pm.[3])

The excitation functions in Figure 3 provide experimental evidence for additional resonant processes above the 2-eV resonance. The onset energies and peak positions of these higher energy bands differ in the C–H (ν_1) and C–C (ν_3) stretch excitation curves, indicating that more than one resonance is involved. The higher lying resonances are much broader than the 2-eV resonance, and the larger widths are probably caused, at least in part, by a substantially shorter lifetimes, expected for energetically higher-lying resonances because of lower barriers toward autodetachment.

A prototypical case for resonant vibrational excitation mediated by an extremely short-lived resonance is the vibrational excitation through the $^2\Sigma_u$ resonance in H_2. A correct resonant description of this process involves a potential curve which is nonlocal, and the result is strongly affected by its large imaginary part.[34] Rationalization of the broad bands in the observed vibrational cross sections of **1** with virtual orbitals is thus even more problematic than for longer-lived resonance at lower energies. (A discussion of problems encountered with very short-lived resonances has also been given by Gallup.[32]) Despite these limitations we observe, however, that Figure 9 shows a gap of more than 2 eV above LUMO and then a cluster of many σ^* orbitals, qualitatively correctly rationalizing the observations. The calculated σ^* orbitals are antibonding either along the C–C or the C–H bonds (but rarely both simultaneously; see the examples in Figure 9). We therefore propose that the broad bands in the vibrational cross

(30) Paddon-Row, M. N.; Jordan, K. D. In *Modern Models of Bonding and Delocalization*; Liebman, J. F., Greenberg, A., Eds.; VCH Publishers: New York and Weinheim, 1988; p 115.
(31) Howard, A. E.; Staley, S. W. In *Resonances*; Truhlar, D. G., Ed.; American Chemical Society: Washington, D.C., 1984. Heinrich, N.; Koch, W.; Frenking, G. *Chem. Phys. Lett.* **1986**, *124*, 20.
(32) Chen, D.; Gallup, G. A. *J. Chem. Phys.* **1990**, *93*, 8893.
(33) Frisch, M. J.; Head-Gordon, M.; Trucks, G. W.; Foresman, J. B.; Schlegel, H. B.; Raghavachari, K.; Robb, M.; Binkley, J. S.; Gonzalez, C.; Defrees, D. J.; Fox, D. J.; Whiteside, R. A.; Seeger, R.; Melius, C. F.; Baker, J.; Martin, R. L.; Kahn, L. R.; Stewart, J. J. P.; Topiol, S.; Pople, J. A. *Gaussian 90*, Revision I; Gaussian, Inc.: Pittsburgh, PA, 1990.
(34) Mündel, C.; Berman, N.; Domcke, W. *Phys. Rev. A* **1985**, *32*, 181.
(35) Schmelzer, A.; Haselbach, E. *Helv. Chim. Acta* **1971**, *54*, 1299. The program has been substantially improved and modernized by T. Bally, S. Matzinger, and B. Albrecht (Fribourg).

sections are caused by overlapping resonances where the wave functions describing the temporarily captured electron resemble the virtual orbitals. The contributions of individual orbitals to the vibrational cross section will be strongly affected by their lifetimes, controlled by the height of the centrifugal barrier and thus by the symmetry and nodal properties. (In particular, the A_1' orbitals, such as the second LUMO, will couple strongly to the s-wave.) The situation is further complicated by possible mixing of resonances with the same symmetry and possible vibronic coupling of resonances of different symmetries. Finally, one may be tempted to interpret some finer details of the excitation functions in Figure 3 using the virtual orbitals. The fact that the onset of the broad band lies lower in the ν_1 excitation curves than in the $2\nu_3$ excitation curve could be explained by the second LUMO a_1', which is antibonding in C-H but not in C-C, and lies well below the other σ^* orbitals (Figure 9). We feel, however, that such assignments remain speculative without better understanding of the relation between higher-lying virtual orbitals and shape resonances.

Visual inspection of the shapes of the σ^* orbitals indicates that a wide range of partial waves will be associated with the different resonances. It is not unreasonable to expect that the resulting angular distribution is almost isotropic.

V. Conclusion

The extraordinary structure of [1.1.1]propellane is reflected in its electronic structure, which is strikingly different from that of a saturated hydrocarbon. The first vertical attachment energy is nearly identical with that of ethene. Similarly, the first triplet band is at nearly the same energy, and even has the same appearance, as the first triplet band in ethene. The shapes of the triplet band, the negative ion band, and the degree and selectivity of resonant vibrational excitation are well in line with a LUMO which is antibonding along the bridging bond. On the other hand, the band which appears to correspond to the dipole-allowed HOMO → LUMO singlet transition is remarkably narrow. Additional bands in vibrational cross section in the 3-15-eV region indicate short-lived shape resonances which we associate with higher-lying σ^* orbitals. These orbitals play an important role in hyperconjugation, and we plan to continue to study them with the same methodology in other, less "exotic" hydrocarbons.

Acknowledgment. We express our sincere appreciation to Professor E. Haselbach for his continuing support and encouragement in the present work. The construction of the spectrometers represents a major effort in terms of development and fabrication of the mechanical and electronical components. These tasks have been accomplished by E. Brosi of the mechanical laboratory and P.-H. Chassot of the electronical laboratory. The present work would not be possible without their exceptional enthusiasm and ingenuity in finding solutions for all the innumerous problems encountered in the course of the construction. We thank T. Bally and P. Jungwirth for help with the Gaussian program and K. Jordan for kind comments on the manuscript. Financial support by the Deutsche Forschungsgemeinschaft is gratefully acknowledged. This work is part of Project 20-28842.90 of the Schweizerischer Nationalfonds zur Förderung der wissenschaftlichen Forschung.

Models for Polysilane High Polymers. 2. Photophysics of Linear Permethylhexasilane: A Low-Lying Franck-Condon Forbidden Excited Singlet State

Ya-Ping Sun and Josef Michl*,[1]

Contribution from the Department of Chemistry and Biochemistry, University of Colorado, Boulder, Colorado 80309-0215. *Received April 9, 1992*

Abstract: The UV absorption properties of Si_6Me_{14} are those expected from an extrapolation from longer chains, but its fluorescence is not. The observations are best accommodated by postulating that the emitting state of Si_6Me_{14} is distinct from the $\sigma\sigma^*$ state that dominates its absorption, in contrast to the situation in $Si_{10}Me_{22}$ and longer oligosilanes. Tentative assignments are considered for the emitting state. The fluorescence quantum yield of Si_6Me_{14} is strongly temperature dependent, suggesting the existence of a thermally activated radiationless decay channel (E_a = 2.1 kcal/mol, $A = 2 \times 10^{12}$ s^{-1}).

Introduction

Polysilanes, a relatively new class of σ-conjugated polymers, have attracted considerable interest.[2-6] Photophysical and photochemical studies have been focusing on their electronic structure, conformation, and photochemical degradation.[7-11]

The quite unique photophysical and photochemical properties of room-temperature polysilane solutions have been interpreted in terms of the segment distribution model.[7,8,10] In this model it is assumed that the polysilane chain consists of a series of approximately planar all-trans segments separated by one or more approximately gauche twists of the backbone and acting as nearly localized chromophores of different length and energy. The inhomogeneous distribution of the chromophoric segments, their spectroscopic properties, and their energy transfer processes are then assumed to dictate the optical properties of polysilane high

(1) The bulk of this work was performed while the authors were still at the Center for Structure and Reactivity, Department of Chemistry and Biochemistry, University of Texas at Austin, Austin, Texas 78712.

(2) Michl, J.; Sun, Y.-P. In *Radiation Effects on Polymeric Materials*; Reichmanis, E., O'Donnell, J. H., Frank, C. W., Eds.; ACS Symposium Series; American Chemical Society: Washington, DC, in press.

(3) Michl, J. *Synth. Met.*, in press.

(4) Miller, R. D.; Michl, J. *Chem. Rev.* **1989**, *89*, 1359.

(5) Zeigler, J. M. *Synth. Met.* **1989**, *28*, C581; *Mol. Cryst. Liq. Cryst.* **1990**, *190*, 265.

(6) West, R. *J. Organomet. Chem.* **1986**, *300*, 327.

(7) (a) Michl, J.; Downing, J. W.; Karatsu, T.; Klingensmith, K. A.; Wallraff, G. M.; Miller, R. D. In *Inorganic and Organometallic Polymers*; Zeldin, M., Wynne, K., Allcock, J., Eds.; ACS Symposium Series 360; American Chemical Society: Washington, DC, 1988, Chapter 5. (b) Klingensmith, K. A.; Downing, J. W.; Miller, R. D.; Michl, J. *J. Am. Chem. Soc.* **1986**, *108*, 7438.

(8) Harrah, L. A.; Zeigler, J. M. *Macromolecules* **1987**, *20*, 601.

(9) (a) Thorne, J. R. G.; Williams, S. A.; Hochstrasser, R. M.; Fagan, P. J. *Chem. Phys.* **1991**, *157*, 401. (b) Thorne, J. R. G.; Repinec, S. T.; Abrash, S. A.; Zeigler, J. M.; Hochstrasser, R. M. *Chem. Phys.* **1990**, *146*, 315.

(10) Sun, Y.-P.; Miller, R. D.; Sooriyakumaran, R.; Michl, J. *J. Inorg. Orgnomet. Polym.* **1991**, *1*, 3.

(11) (a) Michl, J.; Downing, J. W.; Karatsu, T.; McKinley, A. J.; Poggi, G.; Wallraff, G. M.; Sooriyakumaran, R.; Miller, R. D. *Pure Appl. Chem.* **1988**, *60*, 959. (b) Miller, R. D.; Rabolt, J. F.; Sooriyakumaran, R.; Fleming, W.; Fickes, G. N.; Farmer, B. L.; Kuzmany, H. In *Inorganic and Organometallic Polymers*; Zeldin, M., Wynne, K., Allcock, J., Eds.; ACS Symposium Series 360; American Chemical Society: Washington, DC, 1988, Chapter 4.

0002-7863/92/1514-8186$03.00/0